Effects of Sublattice Symmetry and Frustration on Ionic Transport in Garnet Solid Electrolytes

Boris Kozinsky and Sneha A. Akhade
Robert Bosch LLC, Research and Technology Center North America, 255 Main St, Cambridge, Massachusetts 02142, USA

Pierre Hirel
Fraunhofer Institute for Mechanics of Materials IWM, Wöhlerstr. 11, 79108 Freiburg, Germany and Unité Matériaux et Transformations, Bât. C6, Université de Lille 1, 59655 Villeneuve dAscq, France

Adham Hashibon and Christian Elsässer
Fraunhofer Institute for Mechanics of Materials IWM, Wöhlerstr. 11, 79108 Freiburg, Germany

Prateek Mehta
Robert Bosch LLC, Research and Technology Center North America, 255 Main St, Cambridge, Massachusetts 02142, USA

Alan Logeat and Ulrich Eisele
Robert Bosch GmbH, Corporate Sector Research and Advance Engineering, Robert-Bosch-Platz 1, 70839 Gerlingen-Schillerhöhe, Germany

(Received 26 June 2015; published 5 February 2016)

We use rigorous group-theoretic techniques and molecular dynamics to investigate the connection between structural symmetry and ionic conductivity in the garnet family of solid Li-ion electrolytes. We identify new ordered phases and order-disorder phase transitions that are relevant for conductivity optimization. Ionic transport in this materials family is controlled by the frustration of the Li sublattice caused by incommensurability with the host structure at noninteger Li concentrations, while ordered phases explain regions of sharply lower conductivity. Disorder is therefore predicted to be optimal for ionic transport in this and other conductor families with strong Li interaction.

DOI: 10.1103/PhysRevLett.116.055901

Solid-state Li-ion batteries have generated keen interest as advanced energy storage systems with applications in portable electronics and electric vehicles [1]. A highly conductive and stable solid ceramic ionic conductor can enable high-energy density by serving as a protection layer for Li-metal anodes, and a stable electrolyte for high-voltage cathodes. At the same time, replacing flammable organic electrolytes with an inorganic compound will remove the threat of thermal runaway catastrophes. Solid-state inorganic Li conducting oxides with the garnet structure are currently considered to be among the top promising candidates for solid electrolytes due to a combination of their performance and stability properties. The garnetlike conductor $Li_5La_3M_2O_{12}$ ($M = Nb$, Ta) was first reported by Thangadurai *et al.* [2] and to date an ionic conductivity as high as $\sigma = 3 \times 10^{-3}$ S/cm has been measured [3] for the cubic $Li_7La_3Zr_2O_{12}$ garnet. The prototypical garnet structure is cubic (group $Ia-3d$ No. 230) with the chemical formula $Li_xB_3C_2O_{12}$. This structure is remarkably robust in regard to changes in cation composition (B = La, Ca, Ba, Sr, Y, Pr, Nd, Sm-Lu, and C = Zr, Ta, Nb, Nd, Te, W) and is able to accommodate Li concentrations x ranging from 3 to 7. There are two distinct crystallographic Li sites: octahedral (oct) 48g and tetrahedral (tet) 24d. Each tet site shares a face with four oct sites, while each oct site shares a face with two tet sites, thus forming a percolating Li site network. Other cations occupy the 24c (B) and 16a (C) sites, and oxygen occupies the 96h site. It has been recognized that Li site arrangements vary with Li content x, but there are conflicting reports of the trends coming from experimental measurements [4–6]. Li arrangement is difficult to refine, even with neutron scattering, and the nature of ionic conduction is impossible to observe directly. At the same time a complex relationship between crystal structure and conductivity is evident and important for optimizing the materials performance. Multiple phases have been reported across the composition space with widely ranging conductivity values, which depend not only on stoichiometry but also preparation routes. For example, it was reported that $Li_7La_3Zr_2O_{12}$ is tetragonal (t-LLZ) with 2 orders of magnitude lower conductivity than the cubic (c-LLZ) polymorph [7]. In this work we aim to derive a comprehensive description of the atomic mechanisms governing garnet crystals, which is able to explain both structural and dynamic effects in a wide composition space. Towards this goal we develop and employ a combination of computational methods that include systematic hierarchical space

group symmetry analysis coupled with high-throughput atomistic computations and molecular dynamics.

The arrangement of Li ions among the available crystallographic sites is arguably the main degree of freedom that controls both the structure and transport characteristics of the garnet solid electrolytes. However, complete brute-force analysis of Li orderings is impossible due to the complexity of the crystal: for LLZ ($x = 7$) there are 72 Li sites, of which 56 are occupied, resulting in 10^{15} possible arrangements, and 10^{19} for $x = 6$. In order to deal with the enormous combinatorial space of configurations, we combine rigorous group-theoretic analysis for classifying Li site arrangements for each composition together with automated computations of energies using density functional theory (DFT). The resulting complete mapping of lowest energy structures at each composition is then used to predict new ordered or disordered phases of garnets and to postulate the dependency of conductivity on composition. The first step in our analysis is to verify that the occupancy partitioning of Li among tet and oct sites depends only on the overall Li concentration x in the composition. To this end, we generate a set of ~100 candidate configurations of various oct:tet occupancy ratios for a range of x values. Each structure is relaxed using DFT and the occupancy of the lowest energy configuration is automatically extracted by analyzing crystal topology. This procedure involves partitioning of the crystal into a compact geometric network of nonoverlapping polyhedra with oxygen atoms as vertices. Each polyhedron is then analyzed using a convex hull algorithm to determine whether there is a Li ion present within its boundaries. As shown in Fig. 1 the trend is in fact linear, with Li favoring tet site occupancy for low Li concentrations $x < 4.5$. In order to investigate the effects of dynamics

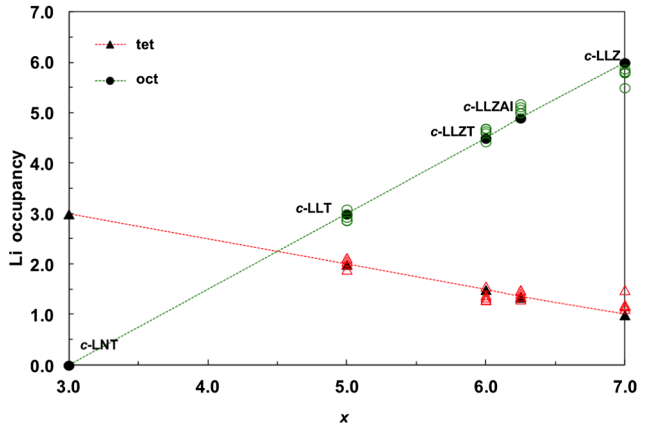

FIG. 1. Linear trend of Li occupancy (black) of oct and tet sites as a function of Li content. Temperature dependent oct (green) and tet (red) Li occupancy (500–1300 K) do not significantly deviate from occupancies at 0 K. Labels denote c, cubic; LLZ, $Li_7La_3Zr_2O_{12}$; LLZAl, $Li_{6.25}Al_{0.75}La_3Zr_2O_{12}$; LLZT, $Li_6La_3ZrTaO_{12}$; LLT, $Li_5La_3Ta_2O_{12}$; LNT, $Li_3Nb_3Te_2O_{12}$.

on this trend we performed *ab initio* molecular dynamics (AIMD) at several temperatures, concluding that entropic effects have a minor effect on the trend. Qualitatively similar results have been observed in several experimental reports [4,5,8,9], but quantitative results vary, likely due to differences in material preparation.

The occupancy constraint allows us to reduce the number of candidate configurations in the search for the ground state at each composition ($3 < x < 7$), but the number of possibilities is still ~10^{17} for $x = 6$. To reduce the number of relevant configurations we perform a systematic search through crystallographic symmetry groups, subject to the constraint of the site occupancy ratio. This enables us to efficiently analyze the entire space of possible ordered ground-state structures in the garnet crystal family, using only a few hundred configurations. The group theoretic analysis procedure starts with crystallographic projections of the prototypical cubic symmetry group $Ia\bar{3}d$ (No. 230) of the host lattice onto lower-symmetry subgroups in order to enumerate ordered structures at partial Li occupancies. The subgroup projection is implemented using tools provided by the Bilbao Crystallographic Server [10] (details in the Supplemental Material [11]). We only consider cubic and tetragonal candidate subgroups, motivated by the experimental observation of only these two lattice types in the garnet family. First, for each Li concentration x, we determine all subgroups of group No. 230 with the k index up to 2. (The k index indicates the multiplication factor relating the volume of the primitive cell of the subgroup with respect to the primitive cell of the original prototype structure.) This limit is imposed in order to limit the search to ordered structures with a reasonably compact description of a highly ordered phase. We then analyze the splittings [22] of Wyckoff positions in each subgroup and conjugacy class in order to identify symmetrically related sets of Li sites and their multiplicities. The oct:tet occupancy ratio constraint is introduced by requiring that each resulting structure accommodates the correct ratio with the available Li site multiplicities. Finally, for each ordered structure that satisfies these constraints we perform DFT variable-cell optimization calculations and identify the Li configuration of lowest energy for each composition x. The main result of this analysis is the nontrivial finding that for each of the integer values of $x = 3, 4, 5, 6, 7$ there exist ordered configurations with cubic or tetragonal symmetry, and that some are more robust than others with respect to the tendency to disorder. In the following, we discuss in detail the Li configurations we identify for each integer concentration x. We note that it is not possible to find ordered structures (within the specified constraints) for noninteger concentrations, so they are predicted to be cubic and disordered.

$x = 7$.—From the subgroup projection procedure, the highest symmetry subgroup that allows for the occupancy ratio of 1:6 (tet:oct) is the tetragonal group $I4_1/acd$

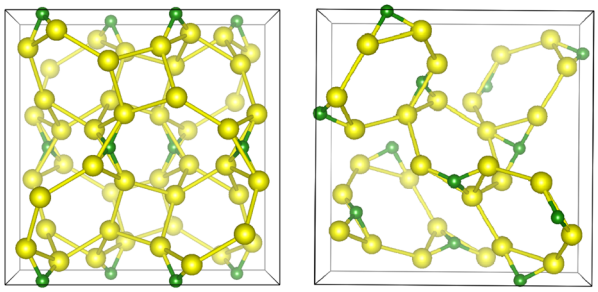

FIG. 2. 3D representation of the ground-state Li arrangement for $x = 7$ (left), $x = 6$ (right). tet Li is represented by green spheres, and oct Li by yellow spheres. The other constituents of the crystal are omitted for ease of viewing.

(No. 142). It is not possible to find any cubic subgroups of group No. 230, subject to the constraints of occupancy and unit cell size. DFT calculations identify the tetragonal layered structure as the lowest energy configuration. In this configuration Li occupies all the oct sites as well as one-third of the tet sites in a characteristic ordered layered arrangement (illustrated in Fig. 2, left), which imparts a noticeable tetragonal distortion ($c/a = 1.04$ for t-LLZ) to the unit cell. XRD/neutron diffraction results [7] confirm the tetragonal nature of the ground-state structure of LLZ, as well as the layered Li atom arrangement. Li in an oct site ($48g$ in the prototype structure) is distorted to occupy the Wyckoff position $96h$ when one of the neighboring tet sites is occupied. This oct site distortion is present in other garnet compositions as well, indicating a significant degree of interaction among Li in the sublattice. The tetragonal structure is quite stationary, which is indicated by the high energy cost to move a Li ion from an oct site to a tet site (~0.7 eV) [23] and the tendency to rearrange subsequently back to the original state. In addition to the tetragonal structure, however, we find multiple low-symmetry configurations with the Li occupancy of 1.5:5.5 (tet:oct), which deviates slightly from the expected occupancy trend. These structures are higher in energy by as little as 5 meV per Li site and the cell shape is much closer to cubic, as expected from lower symmetry configurations. This is consistent with experimental observations that a phase transition can turn the ordered tetragonal LLZ (t-LLZ) to a disordered cubic form (c-LLZ) [24].

$x = 6$.—The occupancy trend predicts a tet:oct ratio 1.5:4.5 for this composition. A representative compound of this composition is $Li_6La_3ZrMO_{12}$, where $M = Nb^{5+}$(LLZN) or Ta^{5+}(LLZT). Symmetry subgroup analysis of Wyckoff position splittings identifies only one possible cubic Group No. 198 ($P2_13$). Within this space group the half-half mixing of cations (Zr:Ta/Zr:Nb) can also be accommodated in several ways. Overall there are 48 structures corresponding to arrangements of Li ions and cations within this space group, and we perform DFT variable-cell relaxation calculations to identify the ground-state configuration for both mixed Zr-Ta and Zr-Nb cation compositions. The lowest energy structure exhibits a rocksalt type ordering of the $4+/5+$ cations, and a simple pattern of Li ions, where each tet Li has exactly 3 oct neighbors (see Supplemental Material [11]). In addition, each tet Li has zero tet neighbors, and exactly half of the tetrahedral sites are occupied (see Fig. 2, right). The excitation energy to disturb the ordering is calculated to be 23 meV/Li site. Although experimental results report that $x = 6$ compositions are indeed cubic [25], a detailed characterization of Li ion arrangement is presently lacking. Our finding presents new information explaining the likely ground-state structure of this composition, which can anticipate confirmation from neutron diffraction studies of carefully annealed samples.

$x = 5$.—The prescribed occupancy ratio of 2:3 (tet:oct) is possible to obtain within the tetragonal group No. 98 ($I4_122$) as the highest symmetry compatible with the Li site Wyckoff position splitting. Group No. 80 ($I4_1$) is a tetragonal subgroup of No. 98, and also accommodates the required occupancy. DFT variable-cell relaxation calculations of $Li_5La_3M_2O_{12}$ ($M = Nb^{5+}$ or Ta^{5+}) identify a tetragonal structure of group No. 98 as the lowest energy configuration. However, we also find multiple tetragonal structures corresponding to space group No. 80 that are only 9 meV per Li site higher in energy than the ground state. We predict that this degeneracy is likely to yield a statistically averaged cubic structure at room temperature with no long range Li order, as synthesized, for this composition [26]. We propose that it may be possible to detect tetragonal domains with sensitive neutron diffraction equipment, for samples annealed at lower temperatures. Similar to the $x = 6$ case, we find that the relative energies of arrangements in $Li_5La_3Ta_2O_{12}$ (LLT) and $Li_5La_3Nb_2O_{12}$ (LLN) garnets are very close, predicting similar structural and transport behavior in these compositions.

$x = 4$.—The tet:oct occupancy ratio of 2.5:1.5 can be accommodated by Wyckoff position splitting in tetragonal groups No. 117, 116, and 95. By computing total energies for each of 142 possible optimized configurations in $Li_4La_3TaWO_{12}$ we find that the lowest energy structures belong to space group No. 95. The one identified as the lowest energy ordered structure is detailed in the Supplemental Material [11]. The next-lowest energy structure in this family is higher in energy by 20 meV/Li site, which also makes it challenging to observe especially if the high-temperature synthesis procedure involves a rapid quenching step. Unless carefully annealed, this composition is likely to be cubic and disordered, as synthesized.

$x = 3$.—In the classical silicate garnet structure (space group No. 230) all the $24d$ sites (tet) are occupied but none of the $48g$ (oct) sites. In the case of Li garnets, our subgroup projection approach identifies a unique structure with group No. 230 as the highest symmetry compatible with full tet occupancy, as dictated by the linear occupancy trend. This

well-ordered cubic structure is strongly favored energetically, requiring more than 1.0 eV of energy to displace a Li ion from its tet position in $Li_3La_3Te_2O_{12}$. Previous neutron diffraction studies [27] have determined the lithium distribution in $Li_3La_3Te_2O_{12}$ and $Li_3Nd_3W_2O_{12}$ and conform to our prediction.

In order to investigate the dependence of ionic conductivity on composition, we compute it using classical molecular dynamics (CMD). In CMD simulations the cell geometry was cubic and the cation composition was La and Zr, with only the Li concentration varied to study its influence on diffusion. CMD activation energies for $x = 5$ and $x = 7$ (c-LLZ) were validated using AIMD and found to be 25% lower, due to approximate potentials used. The emerging picture (Fig. 3) is that both tetragonal and cubic phases appear in the composition range, but the ionic conductivity depends primarily on the degree and robustness of order in the Li sublattice. Indeed, we find clear qualitative features where conductivity is noticeably suppressed for compositions $x = 3, 4, 6, 7$, precisely where well-ordered ground-state Li configurations exist, with non-negligible excitation energies. On the other hand, much shallower energy landscapes results in better ionic mobility in disordered configurations that arise in situations of frustration. At compositions, such as half-integral x, no low-energy Li arrangements exist with symmetry compatible with the host crystal lattice, making the Li network intrinsically frustrated, disordered and mobile. This interplay between carrier lattice symmetry and conductivity is reminiscent of disorder-induced transport observed in frustrated models, e.g., the triangular antiferromagnetic Ising model [28].

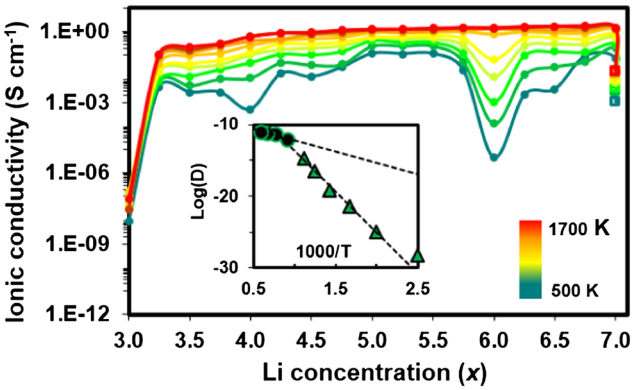

FIG. 3. Ionic conductivity (S/cm) of Li^+ for temperatures 500 to 1700 K as a function of Li content x in the garnet crystal, from CMD simulations. At $x = 7$, the conductivity of the tetragonal (t-Li7) (denoted as hollow squares) and cubic (c-Li7) phases of $Li_7La_3Zr_2O_{12}$ have been depicted. Inset: Logarithm of the diffusion coefficient versus inverse temperature (1000/T in 1/K) for the $x = 6$ structure, illustrating the order-disorder phase transition at about 900 K. Black circles represent high-temperature values and green triangles represent low-temperature values.

In the case of $x = 6$, the newly identified ordered ground-state results in poor mobility at lower temperatures. As depicted in Fig. 3, a decline of ionic motion at even higher temperatures up to 900 K is indicative of Li sublattice configuration freezing, which is confirmed by topological structural analysis. The Arrhenius plot of diffusion coefficients from CMD simulations exhibits a sublattice phase transition where the Li-ion network is mobile at high temperature but freezes into its ground-state configuration at lower temperatures. A relatively low activation energy E_A of 0.27 eV is obtained for high temperatures (1700–1100 K). But for a range of lower temperatures (900–500 K), the E_A computed in CMD reached 0.98 eV. Experimental activation energy may quantitatively vary, depending on the sample preparation procedure of the $x = 6$ crystal, that may result in a partially locked Li arrangement. For concentrations just above and below $x = 6$, mobile defects move freely in the background of the stable configuration, leading to sharp increases of conductivity. In this picture the concentration of free carriers remains smaller that the nominal Li concentration x in this and other composition regions close to an ordered ground state. This consideration explains the recent finding that only about 10% of Li in garnets contribute to conductivity [29], and also suggests that half-integer concentration are optimal for conductivity. For $x = 3$ and $x = 7$ (t-LLZ) the CMD simulations do not show any significant ionic motion even at high temperature, as confirmed also by AIMD. Indeed, for $x = 3$, an ordered disconnected network of only tet Li cannot move because migration to an oct site is very unfavorable. As more Li ions are introduced, they act as free carriers moving in the background of a static high-symmetry $x = 3$ configuration, leading to a rapid increase in conductivity. A similar situation prevails for the fully filled set of oct sites in the ordered tetragonal ground state of $x = 7$ (t-LLZ), where the cost of creating oct vacancies is high. Reducing Li content by adjusting the composition introduces mobile vacancies that increase conductivity. At the same time, a higher degree of motion can also be observed in the "excited" configuration of LLZ with cubic structure c-LLZ and a tet:oct occupancy ratio of 1.5:5.5. In this case oct vacancies are present and act as carriers, and the availability of multiple degenerate configurations leads to disorder and significant freedom of motion. The simulations predict a distinct difference of 1–2 orders of magnitude in the conductivity between the ground state (t-Li7) and the disordered state (c-Li7), consistent with experimental observations [30]. CMD simulations for the case of $x = 5$ exhibit better transport, as compared to the other integer compositions, due to a greater intrinsic propensity towards disorder. This can be attributed to the presence of multiple configurations that are energetically similar to the ground-state arrangement and tend to yield an average low-symmetry configuration. The slight dip of conductivity at

$x = 4$ is again consistent with the presence of an ordered ground state; however, in this case disorder is seen to set in at lower temperatures than for $x = 6$.

In conclusion, we provide the basis for understanding the nontrivial relationship between composition, structure, and transport that governs performance of garnets in the wide range of compositions. Through systematic structural symmetry analysis based on the universal occupancy trend, combined with *ab initio* energy computations, we predict that ordered ground-state crystal structures exist for integer compositions. Some of these structures have been confirmed experimentally, while others are yet to be detected. In particular, we identify ordered ground states at most integer compositions (notably new phases for the $x = 4$ and $x = 6$), and characterize their configurational excitations. The lack of stable ordered states at half-integer concentrations results in disordered frustrated configurations that maximize carrier concentration and mobility. This is a consequence of the strong Li-Li interaction and the particular symmetry structure of the host lattice, and indicates that it is primarily the Li concentration and arrangement that controls transport in garnets. Based on this new understanding, we expect that intrinsic conductivity is highest at compositions around $x = 5.5$ and $x = 6.5$, and that is where future experimental efforts should focus. We speculate that presented methods and understanding are relevant to other families of ionic conductors, where Li concentration is adjustable and Li-Li interaction is strong, such that sublattice frustration and disorder can be used to optimize ionic transport.

This research used resources of the Oak Ridge Leadership Computing Facility which is supported by the Office of Science of the Department of Energy under Contract No. DE-AC05-00OR22725. The part of this work done at Robert Bosch GmbH and Fraunhofer IWM in Germany was funded by the German Federal Ministry of Education and Research BMBF within the Project HE-Lion (Grant No. INLB03088008).

[1] B. Scrosati and J. Garche, J. Power Sources **195**, 2419 (2010).
[2] V. Thangadurai, H. Kaack, and W. J. F. Weppner, J. Am. Ceram. Soc. **86**, 437 (2003).
[3] R. Murugan, V. Thangadurai, and W. Weppner, Angew. Chem., Int. Ed. **46**, 7778 (2007).
[4] H. Xie, J. A. Alonso, Y. Li, M. T. Fernández-Díaz, and J. B. Goodenough, Chem. Mater. **23**, 3587 (2011).
[5] M. P. O'Callaghan, A. S. Powell, J. J. Titman, G. Z. Chen, and E. J. Cussen, Chem. Mater. **20**, 2360 (2008).
[6] T. Thompson, A. Sharafi, M. D. Johannes, A. Huq, J. L. Allen, J. Wolfenstine, and J. Sakamoto, Adv. Energy Mater. **5**, 1500096 (2015).
[7] J. Awaka, N. Kijima, H. Hayakawa, and J. Akimoto, J. Solid State Chem. **182**, 2046 (2009).
[8] E. J. Cussen, J. Mater. Chem. **20**, 5167 (2010).
[9] A. Logéat, T. Köohler, U. Eisele, B. Stiaszny, A. Harzer, M. Tovar, A. Senyshyn, H. Ehrenberg, and B. Kozinsky, Solid State Ionics **206**, 33 (2012).
[10] M. I. Aroyo, J. M. Perez-Mato, D. Orobengoa, E. Tasci, G. de la Flor, and A. Kirov, Bulg. Chem. Commun. **43**, 183 (2011).
[11] See Supplemental Material at http://link.aps.org/supplemental/10.1103/PhysRevLett.116.055901 for computational details and structure information, which contains Refs. [12–21].
[12] P. Giannozzi *et al.*, J. Phys. Condens. Matter **21**, 395502 (2009).
[13] S. Plimpton, J. Comput. Phys. **117**, 1 (1995).
[14] D. Vanderbilt, Phys. Rev. B **41**, 7892 (1990).
[15] J. P. Perdew, M. Ernzerhof, and K. Burke, J. Chem. Phys. **105**, 9982 (1996).
[16] C. G. Broyden, IMA J. Appl. Math. **6**, 76 (1970).
[17] R. Fletcher, Computer Journal (UK) **13**, 317 (1970).
[18] L. Verlet, Phys. Rev. **159**, 98 (1967).
[19] W. G. Hoover, Phys. Rev. A **31**, 1695 (1985).
[20] T. S. Bush, J. D. Gale, C. R. A. Catlow, and P. D. Battle, J. Mater. Chem. **4**, 831 (1994).
[21] S. M. Woodley, P. D. Battle, J. D. Gale, and C. R. A. Catlow, Phys. Chem. Chem. Phys. **1**, 2535 (1999).
[22] E. Kroumova, J. M. Perez-Mato, and M. I. Aroyo, J. Appl. Crystallogr. **31**, 646 (1998).
[23] K. Meier, T. Laino, and A. Curioni, J. Phys. Chem. C **118**, 6668 (2014).
[24] N. Bernstein, M. D. Johannes, and K. Hoang, Phys. Rev. Lett. **109**, 205702 (2012).
[25] J. Awaka, N. Kijima, Y. Takahashi, H. Hayakawa, and J. Akimoto, Solid State Ionics **180**, 602 (2009).
[26] H. Peng, Q. Wu, and L. Xiao, J. Sol-Gel Sci. Technol. **66**, 175 (2013).
[27] M. P. O'Callaghan, D. R. Lynham, E. J. Cussen, and G. Z. Chen, Chem. Mater. **18**, 4681 (2006).
[28] D. Novikov, B. Kozinsky, and L. Levitov, Phys. Rev. B **72**, 235331 (2005).
[29] H. Nozaki, M. Harada, S. Ohta, I. Watanabe, Y. Miyake, Y. Ikedo, N. H. Jalarvo, E. Mamontov, and J. Sugiyama, Solid State Ionics **262**, 585 (2014).
[30] J. Awaka, A. Takashima, K. Kataoka, N. Kijima, Y. Idemoto, and J. Akimoto, Chem. Lett. **40**, 60 (2011).